Organic LETTERS

Letter

pubs.acs.org/OrgLett

Reductive Benzylation of C_{60} Imidazoline with a Bulky Addend

Hui-Lei Hou, Zong-Jun Li, and Xiang Gao*

State Key Laboratory of Electroanalytical Chemistry, Changchun Institute of Applied Chemistry, University of the Chinese Academy of Sciences, Chinese Academy of Sciences, 5625 Renmin Street, Changchun, Jilin 130022, China

Supporting Information

ABSTRACT: Reductive benzylation of C_{60} imidazoline with a bulky addend affords two 1,2,3,16-adducts (**2** and **4**) and one 1,2,3,4-adduct (**3**). Experimental and computational results indicate that the sterically favored **2** is more stable than the electronically favored **3**. However, an opposite stability order is shown for the dianions of **2** and **3**.

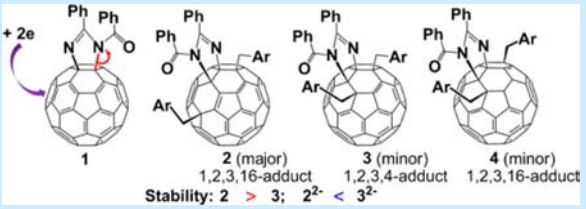

Rearrangement of the cyclic addends on the surface of fullerene cages is of interest, as it may reveal insights on fullerene reactivity and result in novel fullerene derivatives, like the cases of C_{60} tetrazines[1] and fullerene oxazolines.[2] However, the types of fullerene derivatives reported for rearrangement so far are very limited;[1,2] studies are more focused on compounds with the less steric demanding addends where the electronically favored 1,2,3,4-adducts are typically obtained,[1,2] while less is known when the steric demanding addends are involved.

Fullerene imidazolines are a type of compound where the amidine functional group is bonded to a fullerene cage (Scheme 1).[3] They are likely to undergo reductive heterocyclic cleavage

Scheme 1. Illustrated Structures of 1−4

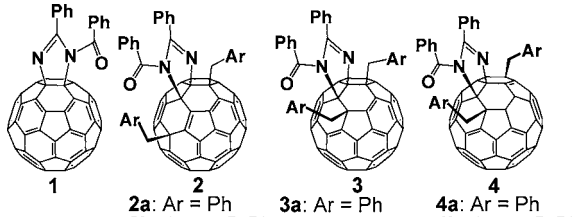

due to the presence of the polar C_{60}−N bond. Among the C_{60} imidazolines, compound **1** (Scheme 1) is of particularly interest since it bears a bulky cyclic addend congested with two phenyl rings.[3b] Herein, we report the reductive imidazoline cleavage of compound **1**, and the unusual formation of three regioisomers **2**, **3** and **4** (Scheme 1) by benzylation of the ring-opened dianion of **1** as a result of both the steric and electronic effects. In addition, a stability reversal is shown for the neutral and dianionic species of **2** and **3**, demonstrating an interesting difference between the electronic and steric factors.

Compound **1** was obtained with procedures reported previously.[3b] Figure 1 shows the cyclic voltammograms of the neutral, singly, and doubly reduced species of **1**. The first redox wave of neutral **1** is quasi-reversible with $E_{1/2}$ at −0.48 V vs SCE, suggesting that the monoanion of **1** is likely stable. The second redox wave appears with $E_{1/2}$ at −0.86 V; however, it

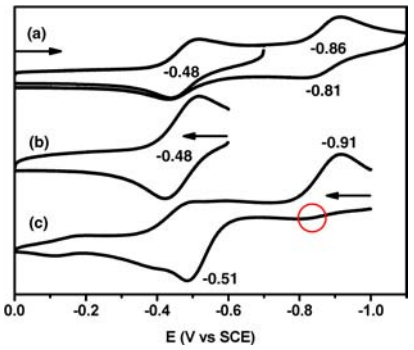

Figure 1. Cyclic voltammograms of (a) **1**, (b) $\mathbf{1}^{-}$, and (c) $\mathbf{1}^{2-}$ in benzonitrile containing 0.1 M TBAP at rt. Scan rate = 0.1 V/s. The arrows indicate the starting potentials and the scan direction for the cyclic voltammetric measurements.

exhibits an irreversibility nature as evidenced by the slight decrease of the anodic current compared with the cathodic current, suggesting that a chemical process likely occurs in $\mathbf{1}^{2-}$. The stability of $\mathbf{1}^{\bullet-}$ is confirmed by the in situ cyclic voltammogram of the species (Figure 1b),[4] where a quasi-reversible redox wave is shown with $E_{1/2}$ identical to that for the neutral compound. In contrast, the cyclic voltammogram of the in situ generated $\mathbf{1}^{2-}$ displays an irreversible redox wave,[5] where the expected anodic peak at −0.81 V (see Figure 1a) has almost completely vanished (red cycle in Figure 1c) as the potential is scanned starting from −1.00 V toward the positive potential. Instead, a new strong anodic wave appears at −0.51 V, which likely corresponds to the oxidation process of $\mathbf{1}^{2-}$ and is coupled with the cathodic peak at −0.91 V judging from the peak currents. The cyclic voltammogram of $\mathbf{1}^{2-}$ is similar to that of C_{60} oxazoline dianion, which undergoes a heterocyclic ring-opening by cleaving the C_{60}−O bond,[2a] suggesting that the imidazoline heterocycle probably experiences a similar ring-opening process upon receiving two electrons. The heterocyclic

Received: November 22, 2013
Published: January 30, 2014

   dx.doi.org/10.1021/ol403395r | *Org. Lett.* 2014, 16, 712−715

cleavage in 1^{2-} is further confirmed by the vis-near IR spectrum (Figure S1, Supporting Information), where absorptions typical for RC_{60}^- species (R = neutral or monoanionic group) are shown at around 650, 722, and 979 nm,[6] suggesting that not only one of the C_{60}–N bonds is cleaved but the cleaved nitrogen atom also carries one negative charge, as the C_{60} cage bears only one charge.

Benzylation of 1^{2-} with $ArCH_2Br$ (Ar = Ph and *o*-BrPh, 60 equiv to **1**) was performed in order to obtain a better understanding of the reductive imidazoline cleavage on the C_{60} surface. Interestingly, three regioisomers are obtained, and they are designated as **2** (1,2,3,16-adduct), **3** (1,2,3,4-adduct), and **4** (1,2,3,16-adduct), respectively.[7] The 1,2,3,4-configuration (cis-1 configuration) is the most electronically favored structure for C_{60} bisadducts due to the absence of the [5,6]-double bond,[8] which is predicted to increase the system energy by about 8.5 kcal/mol.[9] The 1,2,3,16-adduct (containing one [5,6]-double bond) is sterically favored and is obtained only when there exist sterically demanding addends.[10] Compound **2** is obtained as the predominant product from the reaction, while compounds **3** and **4** are obtained only as the minor products (see Figures S2 and S23, Supporting Information, for HPLC traces. Isolated yield: 34%, 7%, and 3% for **2a**, **3a**, and **4a**, Ar = Ph; 46%, 5%, and 5% for **2b**, **3b**, and **4b**, Ar = *o*-BrPh), suggesting that both the steric and electronic effects affect the formation of the products.

Figure 2 shows the X-ray crystal structure of **2b** along with the selected bond lengths. The crystals are composed of a 50:50

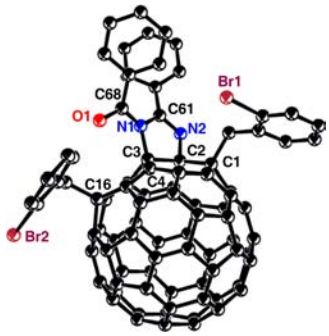

Figure 2. ORTEP diagram of **2b** with 50% thermal ellipsoids. Hydrogen atoms and solvent molecules are omitted for clarity. Selected bond lengths (Å): O1–C68, 1.200(7); N1–C68, 1.389(7); N1–C61, 1.410(7); N1–C3, 1.500(7); N2–C61, 1.288(7); N2–C2, 1.471(7); C2–C3, 1.642(7).

mixture of two mirror-image enantiomers which are designated as 1,2,3,16 and 1,2,12,29 in IUPAC terminology.[7] Compared with the structure of **1**,[3b] the imidazoline heterocycle is relocated from a [6,6]-bond in **1** to a [5,6]-bond in **2b**, confirming that one of the N–C_{60} bonds is cleaved in 1^{2-}. The structure also shows that one benzyl is located next to the imino N–C_{60} bond, while the other benzyl is positioned with a 1,4-pattern with respect to the amino N–C_{60} bond in **2b**. The structures of **2a** and **2b** are further characterized by the HRMS, UV–vis, ^{1}H, ^{13}C, and HMBC NMR spectroscopies (Figures S3–S7 and S24–S27, Supporting Information). As for **2a**, it exhibits similar UV–vis, ^{1}H NMR, and ^{13}C NMR spectra to those of **2b**, indicating that **2a** has the same structure as **2b**. Notably, the HMBC NMR of **2a** (Figure S7, Supporting Information) shows a three-bond coupling ($^3J_{CH}$) of the imino nitrogen-bonded sp^3 C_{60} carbon (~91 ppm) with the neighboring methylene protons, in agreement with the structural assignment of **2a**.

The structures of **3a** and **3b** (1,2,3,4-adducts) are established on the basis of spectroscopic characterizations (Figures S10–S14 and S28–S31, Supporting Information). The key evidence arises from the HMBC NMR and UV–vis spectroscopies. The HMBC NMR spectrum of **3a** (Figure S14, Supporting Information) shows that the two nitrogen-bonded sp^3 C_{60} carbon atoms (91 and 87 ppm) are each correlated with one set of methylene protons through a three-bond correlation, indicating explicitly that each benzyl is positioned next to the respective N–C_{60} bond, and **3a** is a 1,2,3,4-adduct. As for **3b**, it not only exhibits ^{1}H and ^{13}C NMR spectra (Figures S30 and S31, Supporting Information) similar to those of **3a** (Figures S12 and S13, Supporting Information), but also UV–vis absorptions (Figure S28, Supporting Information) resembling those of **3a** (Figure S10, Supporting Information), with the characteristic band at around 430 nm for the 1,2,3,4-adducts,[10,11] confirming that **3b** is also a 1,2,3,4-adduct. Notably, the X-ray single-crystal structures of the 1,2,3,4-adducts of C_{60} have been reported,[1,11b] where relocation of the heterocycle from a [6,6]-bond to a [5,6]-bond on the C_{60} surface has also occurred.

Compounds **4a** and **4b** are shown to be another type of 1,2,3,16-adduct. The first evidence is from the UV–vis spectra of **4a** and **4b** (Figures S17 and S32, Supporting Information), which exhibit similar absorptions to those of **2a** and **2b** (Figures S3 and S24, Supporting Information). The results indicate that **4a** and **4b** are also 1,2,3,16-adducts, even though they would have a different structure from that of **2a** and **2b** due to the difference in the ^{1}H and ^{13}C NMR spectra, because the UV–vis absorptions are sensitive toward the addition patterns of fullerene derivatives.[12] Further evidence arises from the HMBC NMR of **4a** (Figure S21, Supporting Information), which shows that one set of methylene protons are correlated with one of the nitrogen-bonded sp^3 C_{60} carbon atoms (~87 ppm), while no correlation is shown between the other set of methylene protons and the other nitrogen-bonded sp^3 C_{60} carbon (~83 ppm). Considering the fact that benzyls are usually added to C_{60} with either 1,2- or 1,4-manner,[13,14] the only possible structure for **4a** and **4b** is the one in which one benzyl is para added with respect to the imino N–C_{60} bond, while the other benzyl is ortho added with respect to the amino N–C_{60} bond, just opposite to the addition patterns of benzyls in **2a** and **2b**. Notably, the HMBC NMR indicates that different from compounds **2** and **3**, the imino nitrogen-bonded sp^3 C_{60} carbon is resonating at upper field (~83 ppm), while the amino nitrogen-bonded sp^3 C_{60} carbon is resonating at lower field (~87 ppm) for **4**. Such a resonance variance is likely caused by different addition patterns of the benzyls, which have been shown to significantly affect the chemical shift of the sp^3 C_{60} carbon as in the case of 1,2- and 1,4-Bn_2C_{60},[14] and is in agreement with the chemical shift for the amino nitrogen-bonded sp^3 C_{60} carbon with a para or ortho added benzyl in **2** or **3** (75 vs 87 ppm).

Stepwise addition of $PhCD_2Br$ and $PhCH_2Br$ was performed in order to differentiate the benzyls added during different steps.[2,15] The experiment was first carried out by adding equal amount of $PhCD_2Br$ and $PhCH_2Br$ ($n_{PhCD2Br}$:$n_{PhCH2Br}$:n_1 = 30:30:1) simultaneously into the solution of 1^{2-}. The ^{1}H NMR spectra of the partially deuterated products **2aI** and **3aI** show almost identical intensity for all the methylene protons (Figures S8 and S15, Supporting Information),[16] which is consistent

dx.doi.org/10.1021/ol403395r | *Org. Lett.* 2014, 16, 712–715

with the results on benzylation of other dianionic fullerene species,[15] indicating that the intensity of the methylene protons added during different steps would be unlikely affected by the secondary kinetic isotope effect (if there is any) during the benzylation of $\mathbf{1}^{2-}$. Then the reaction was carried out by first adding $PhCD_2Br$, followed by adding equal amount of $PhCH_2Br$ ($n_{PhCD2Br}$:$n_{PhCH2Br}$:n_1 = 30:30:1) with a time interval of 3 min, which resulted in the partially deuterated products **2aII**, **3aII** and **4aII**.

The ^{1}H NMR spectra of **2aII** and **3aII** (Figures S9 and S16, Supporting Information) show that for both compounds the intensity of the AB quartet coupled with the sp^3 C_{60} carbon (91 ppm) bonded to the imino nitrogen is significantly weaker than that of the other AB quartet, demonstrating unambiguously that the benzyl next to the imino N−C_{60} bond is the one added during the first step, while the other benzyl located at the para or ortho site with respect to the amino N−C_{60} bond in **2** or **3** is the one added during the second step. For a singly bonded RC_{60}^- intermediate, the subsequent addition would typically take place at either the ortho or para site with respect to the existing addend as a result of the charge distribution and steric effect.[13] The fact that the first added benzyl is located at the ortho site with respect to the imino N−C_{60} bond shows specifically that the imino N−C_{60} bond is the one that remains intact in $\mathbf{1}^{2-}$, while the amino N−C_{60} bond is the one that is cleaved during the reductive ring-opening.

The ^{1}H NMR of **4aII** (Figure S22, Supporting Information), however, shows a totally different scenario. The AB quartet free of coupling with any nitrogen-bonded sp^3 C_{60} carbon has a less intensity compared with the AB quartet that is coupled with one of the nitrogen-bonded sp^3 C_{60} carbon atoms, indicating that the benzyls are para added with respect to the imino N−C_{60} bond during the first step, and are ortho added with respect to the imino N−C_{60} bond during the second step for the formation of **4**, consistent with the cleavage of the amino N−C_{60} bond in $\mathbf{1}^{2-}$ and the structural assignment of **4**.

A plausible mechanism for the reaction of $\mathbf{1}^{2-}$ with $ArCH_2Br$ is shown in Scheme 2. The amino N−C_{60} bond is cleaved after

Scheme 2. Proposed Mechanism for the Reaction of C_{60} Imidazoline Dianion with $ArCH_2Br$

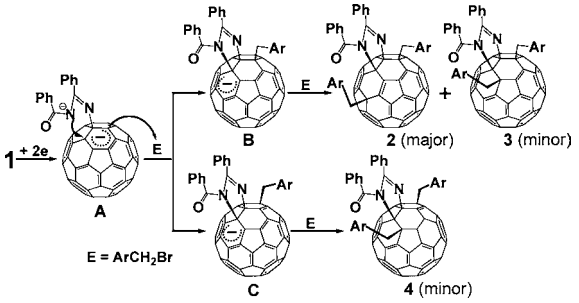

1 receives two electrons, with one electron located at the C_{60} cage and the other one at the amino nitrogen atom in intermediate **A** ($\mathbf{1}^{2-}$) (Figure S36, Supporting Information). The addition of the first benzyl preferably takes place at the ortho carbon ([6,6]-bond) with respect to the remaining imino N−C_{60} bond in **A**, due to the location of the largest negative charge (−0.168) at this carbon as predicted by the NBO analysis at Hartree−Fock (HF)/6-311G(d) level (Figure S37, Supporting Information). In the meantime, a small amount of benzyls are para added with respect to the singly bonded imino N−C_{60} bond, due to the steric effect and also the location of the second largest negative charge (−0.159) at this site (Figure S37, Supporting Information).[13] The addition of the first benzyl is accompanied by the ring-closure of the heterocycle at the [5,6]-bond via the nucleophilic attack of the anionic amino nitrogen to C_{60}, and results in intermediates **B** and **C**. As for the addition of the second benzyl to **B**, the 1,4-addition of the benzyl with respect to the amino N−C_{60} bond is more favorable than the 1,2-addition due to the strong steric effect from the congested benzoyl phenyl ring. Consequently, compound **2** is obtained as the predominant product. In addition, a small amount of benzyls may undergo the 1,2-addition with respect to the amino N−C_{60} bond during the second addition to **B**, as the ortho carbon is predicted to bear a much greater negative charge than the para carbon, (−0.285 vs −0.172, Figure S39, Supporting Information), which would result in **3** as a minor product. As for the addition of the second benzyl to intermediate **C**, the electronic factor may be more important as the para addition of the first benzyl may help to relieve some steric congestion, and it would result in compound **4** due to the location of a greater negative charge at the ortho carbon than at the para carbon with respect to the amino N−C_{60} bond in **C** (−0.290 vs −0.154, Figure S41, Supporting Information). In addition, theoretical calculations predict that **2a** is more stable than **3a** and **4a** by 6.0 and 6.7 kcal/mol (−3530.4825, −3530.4729, and −3530.4718 hartree for **2a**, **3a** and **4a** respectively), consistent with the experimental results.

The electrochemical property of **2** and **3** (1,2,3,16- and 1,2,3,4-adducts) are examined by the cyclic voltammetry. Figure 3 displays the cyclic voltammograms of **2a** and **3a**, where two

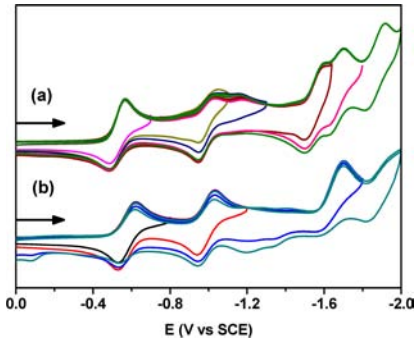

Figure 3. Cyclic voltammograms of (a) **2a** and (b) **3a** in benzonitrile containing 0.1 M TBAP at rt. Scan rate = 0.1 V/s. The arrows indicate the starting potentials and the scan direction for the cyclic voltammetric measurements.

interesting features are noted. First, **2a** exhibits a stronger electron-deficiency than **3a** by showing a more positive $E_{1/2}$ potential for the first redox wave (−0.52 vs −0.58 V vs SCE). Such a strong electron affinity for **2a** is associated with the [5,6]-double bond in the compound as previous work indicates.[17] Second, the 1,2,3,4-adduct (**3a**) shows a more stable electrochemical behavior than the 1,2,3,16-adduct (**2a**), which is somehow surprising since an opposite stability order is observed for the neutral compounds. Both the mono- and dianionic species of **3a** are stable on the time frame of cyclic voltammetry, while only the monoanion of **2a** is stable under the same condition; further reductions result in a more complicated voltammogram for **2a** compared with that of **3a**. Similar results are observed for the cyclic voltammograms of **2b** and **3b** (Figure S42, Supporting Information).

dx.doi.org/10.1021/ol403395r | Org. Lett. 2014, 16, 712−715

The results indicate that the stability of anionic fullerene derivatives is dependent on the electronic structure rather than the steric factor, even though the steric factor significantly affects the stability of the neutral derivatives. Figure 4 depicts

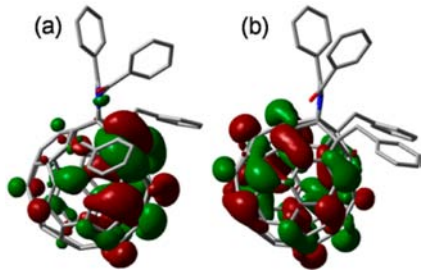

Figure 4. Calculated HOMOs at an isosurface value of 0.02 for (a) $\mathbf{2a}^{2-}$ and (b) $\mathbf{3a}^{2-}$.

the calculated HOMO plots of $\mathbf{2a}^{2-}$ and $\mathbf{3a}^{2-}$, and a notable difference is shown. For $\mathbf{2a}^{2-}$ (1,2,3,16-adduct), the electron cloud of the HOMO, which is consisted of the two extra electrons by reduction, is mainly localized at the C_{60} hemisphere having the [5,6]-double bond; while the HOMO is delocalized over the entire C_{60} surface for $\mathbf{3a}^{2-}$ (1,2,3,4-adduct). Apparently, the presence of the [5,6]-double bond significantly affects the HOMO distributions of C_{60} derivatives. It would result in a congestion of the negative charges within a region in close proximity to the imidazoline heterocycle in $\mathbf{2a}^{2-}$, which would likely destabilize the species as the heterocycle is subjected to reductive cleavage.

In summary, the selective cleavage of the amino N−C_{60} bond is identified for the reductive ring-opening of C_{60} imidazoline. Benzylation of the sterically demanding $\mathbf{1}^{2-}$ results in three regioisomers, with one of the sterically favored 1,2,3,16-regioisomers as the major product, while the electronically favored 1,2,3,4-regioisomer and the other type of 1,2,3,16-regioisomer as the minor products, demonstrating that both the electronic and steric factors affect the formation of fullerene derivatives. Surprisingly, the electrochemical study reveals that the dianion of the less stable 1,2,3,4-adduct (**3**) exhibits a higher stability than that of the more stable 1,2,3,16-adduct (**2**), indicating that the stability of anionic fullerene derivatives is more dependent on the electronic structure, while the steric factor has a much less effect.

■ ASSOCIATED CONTENT

Supporting Information

Experimental and calculation details, crystallographic data (CIF), HPLC traces, and spectra of new compounds. This material is available free of charge via the Internet at http://pubs.acs.org.

■ AUTHOR INFORMATION

Corresponding Author

*E-mail: xgao@ciac.ac.cn.

Notes

The authors declare no competing financial interest.

■ ACKNOWLEDGMENTS

This work was supported by the NSFC (21172212 for X.G., 21202157 for Z.J.L.) and the Solar Energy Initiative of the Chinese Academy of Sciences (KGCX2-YW-399+9).

■ REFERENCES

(1) (a) Miller, G. P.; Tetreau, M. C.; Olmstead, M. M.; Lord, P. A.; Balch, A. L. *Chem. Commun.* **2001**, 1758. (b) Murata, Y.; Suzuki, M.; Rubin, Y.; Komatsu, K. *Bull. Chem. Soc. Jpn.* **2003**, *76*, 1669.

(2) (a) Yang, W.-W.; Li, Z.-J.; Li, F.-F.; Gao, X. *J. Org. Chem.* **2011**, *76*, 1384. (b) Ni, L.; Yang, W.-W.; Li, Z.-J.; Wu, D.; Gao, X. *J. Org. Chem.* **2012**, *77*, 7299.

(3) (a) He, C.-L.; Liu, R.; Li, D.-D.; Zhu, S.-E.; Wang, G.-W. *Org. Lett.* **2013**, *15*, 1532. (b) Hou, H.-L.; Li, Z.-J.; Li, S.-H.; Chen, S.; Gao, X. *Org. Lett.* **2013**, *15*, 4646. (c) Yang, H.-T.; Liang, X.-C.; Wang, Y.-H.; Yang, Y.; Sun, X.-Q.; Miao, C.-B. *Org. Lett.* **2013**, *15*, 4650.

(4) The singly reduced species of **1** ($\mathbf{1}^{\bullet-}$) was generated by the controlled-potential bulk electrolysis at −0.60 V vs SCE.

(5) The doubly reduced species of **1** ($\mathbf{1}^{2-}$) was in situ generated by controlled-potential bulk electrolysis at −1.00 V vs SCE.

(6) (a) Murata, Y.; Motoyama, K.; Komatsu, K.; Wan, T. S. M. *Tetrahedron* **1996**, *52*, 5077. (b) Yang, W.-W.; Li, Z.-J.; Gao, X. *J. Org. Chem.* **2010**, *75*, 4086. (c) Chang, W.-W.; Li, Z.-J.; Yang, W.-W.; Gao, X. *Org. Lett.* **2012**, *14*, 2386. (d) Liu, R.; Li, F.; Xiao, Y.; Li, D.-D.; He, C.-L.; Yang, W.-W.; Gao, X.; Wang, G.-W. *J. Org. Chem.* **2013**, *78*, 7093.

(7) For numbering of C_{60}, see: Godly, E. W. T. R. *Pure Appl. Chem.* **1997**, *69*, 1411.

(8) Hirsch, A.; Brettreich, M. *Fullerenes: Chemistry and Reactions*; Wiley-VCH: Weinheim, 2005.

(9) Matsuzawa, N.; Dixon, D. A.; Fukunaga, T. *J. Phys. Chem.* **1992**, *96*, 7594.

(10) Rubin, Y.; Ganapathi, P. S.; Franz, A.; An, Y.-Z.; Qian, W.; Neier, R. *Chem.—Eur. J.* **1999**, *5*, 3162.

(11) (a) Sander, M.; Jarrosson, T.; Chuang, S.-C.; Khan, S. I.; Rubin, Y. *J. Org. Chem.* **2007**, *72*, 2724. (b) Zheng, M.; Li, F.-F.; Ni, L.; Yang, W.-W.; Gao, X. *J. Org. Chem.* **2008**, *73*, 3159. (c) Tzirakis, M. D.; Alberti, M. N.; Orfanopoulos, M. *Org. Lett.* **2011**, *13*, 3364.

(12) Smith, A. B., III; Strongin, R. M.; Brard, L.; Furst, G. T.; Romanow, W. J.; Owens, K. G.; Goldschmidt, R. J.; King, R. C. *J. Am. Chem. Soc.* **1995**, *117*, 5492.

(13) Subramanian, R.; Kadish, K. M.; Vijayashree, M. N.; Gao, X.; Jones, M. T.; Miller, M. D.; Krause, K. L.; Suenobu, T.; Fukuzumi, S. *J. Phys. Chem.* **1996**, *100*, 16327.

(14) Zheng, M.; Li, F.; Shi, Z.; Gao, X.; Kadish, K. M. *J. Org. Chem.* **2007**, *72*, 2538.

(15) (a) Chang, W.-W.; Li, Z.-J.; Gao, X. *Org. Lett.* **2013**, *15*, 1642. (b) Li, S.-H.; Li, Z.-J.; Yang, W.-W.; Gao, X. *J. Org. Chem.* **2013**, *78*, 7208.

(16) The ^{1}H NMR of **4aI** was not examined due to the low yield of the product.

(17) Popov, A. A.; Kareev, I. E.; Shustova, N. B.; Stukalin, E. B.; Lebedkin, S. F.; Seppelt, K.; Strauss, S. H.; Boltalina, O. V.; Dunsch, L. *J. Am. Chem. Soc.* **2007**, *129*, 11551.